01 Jan 2004

THE PROPERTIES OF BRIDGESTONE ECOPIA SOLAR CAR TIRES (FOR THE UMR SOLAR CAR TEAM)

Tessa C. Russell

THE PROPERTIES OF BRIDGESTONE ECOPIA SOLAR CAR TIRES (FOR THE UMR SOLAR CAR TEAM)

Tessa C Russell
Department of Mechanical Engineering

Abstract
Much of the energy used by a solar car can be attributed to overcoming rolling resistance, and rolling resistance comes predominantly from the tires. The main goal of this project was to better understand the properties of the Bridgestone Ecopia tires used by the UMR Solar Car Team. Experiments were conducted to obtain this objective, measuring the vertical stiffness, lateral stiffness, and contact patch shape and area. As expected, with decreasing pressure and increasing load, the vertical and lateral deflections increased as well as the tire contact patch area.
The stiffness parameters of the tire, measured experimentally were used in an existing rolling resistance model for tires to measure quantitatively how load, pressure and tire misalignment affects the rolling resistance coefficient (C_{rr}) for the tires. With increasing values of the misalignment angle, the coefficient of rolling resistance increased. It was found that a tire can have a larger misalignment angle at higher loads and higher pressures. It was found that load and pressure had the same effect on the coefficient of rolling resistance. The main conclusion that can be reached from the C_{rr} results is that the tires should not have a misalignment angle greater than 1 degree to keep the C_{rr} down.

Introduction
Nearly 35% of the energy used by a well-designed solar car traveling at 56mph can be attributed to overcoming rolling resistance (1). This percentage increases with decreasing speed. The primary factor in rolling resistance is the tires. Therefore it is very important to understand the properties of the tires. There has been very little testing done on the Bridgestone Ecopia tires used by the UMR Solar Car Team. The main goal of this project is to better understand the properties of these Bridgestone Ecopia tires. There are two objectives to reach this goal. The first was to see how the tire deflected vertically with increased load. The second was to be able to better describe the coefficient of rolling resistance of the tires.

Experimental Setup and Procedure
For all experiments, one worn Bridgestone Ecopia tire and one new Bridgestone Ecopia tire, still with a sticker, were used. The following pressures were tested for each tire: 80psi, 100psi, and 120psi.

Tire Vertical Stiffness
The tire was placed in the Instron 5583 between the two compression platens. The Instron Merlin software was then programmed to conduct a compression test with a maximum load of 250lbs and a speed of 0.1in/min. The tire was then loaded per the program three times. The tire was rotated 60degrees for each run. Load and vertical deflection data was collected for each run.

Tire Lateral Stiffness
The tire was placed in the Instron 5583 between the two compression platens. A Linear Variable Differential Transformer (LVDT) was placed at the bottom of the tire, more specifically at the center of the tire wall, which was used to measure lateral deflection. The tire was then compressed to 200lbs. At each pressure, a 35lb lateral load was put on the tire three times. Before and after each lateral load, a lateral deflection was measured. Figure 1 displays the setup of the experiment.

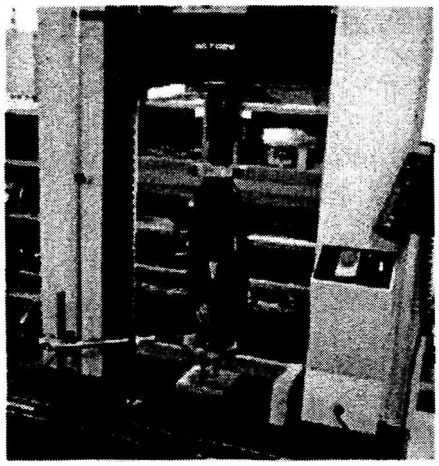

Figure 1: Experimental Setup

Tire Contact Patch

Before the tire was placed in the Instron 5583, three layers were placed on the bottom compression platen. The layers were as follows, bottom first: white computer paper, carbon paper, and 60 grit sandpaper. The tire was then placed in the Instron 5583 between the two compression platens. The tire was then compressed to 150lbs, 175lbs, 200lbs, 225lbs, and 250lbs. Elliptical imprints were made on each piece of white paper, and approximate measurements were taken for the two diameters of the ellipse. Three runs were conducted at each load.

Results and Discussion

Tire Vertical Stiffness

Once the data was collected, for each pressure a graph of load versus vertical deflection was created using Microsoft Excel. To create the graph, the total vertical deflection was divided by two since the measured vertical deflection was the deflection of two sides of the tire rather than one. Figure 1 shows the graph of load versus vertical deflection for the old tire at 80psi. As was expected, the vertical deflection increased with increasing load for each of the three runs.

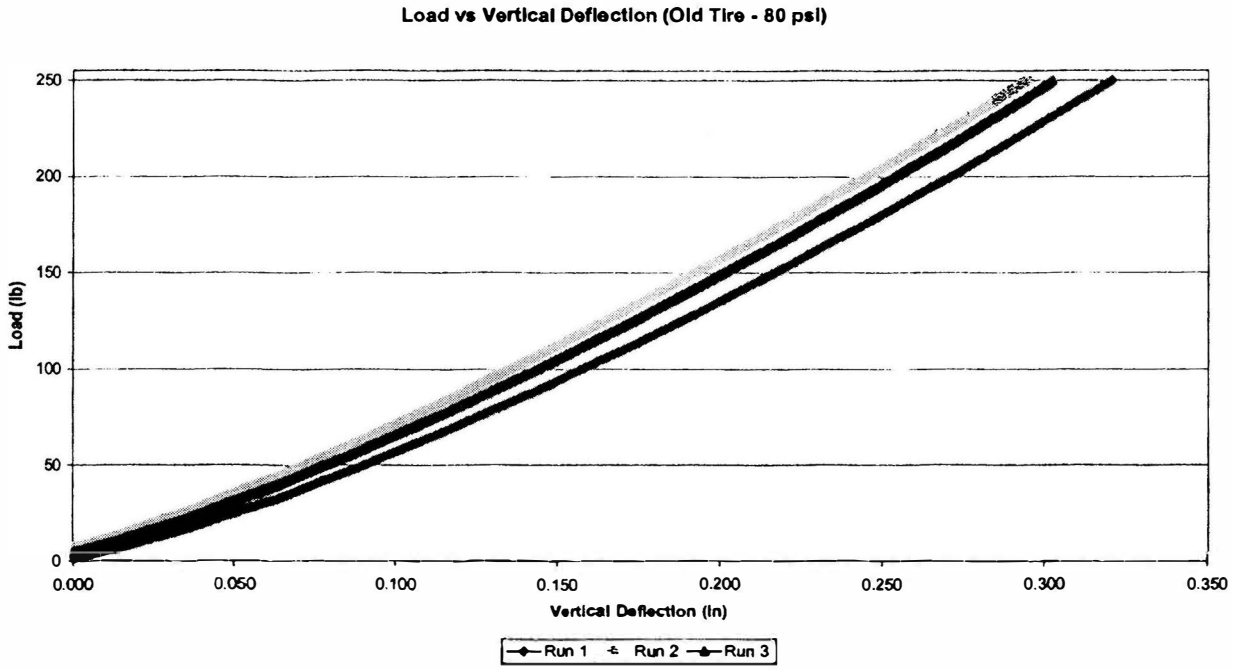

Figure 2: Load vs Vertical Deflection (Old Tire - 80psi)

Similar graphs were seen for pressures of 100psi and 120psi as well as for all pressure graphs for the new tire. As the pressure increased for both the old and new tire, the maximum vertical deflection reached decreased. Table 1 displays the average maximum vertical deflection at 240lbs for both the old and new tire at pressures of 80psi, 100psi, and 120psi.

Table 1: Maximum Vertical Deflection vs Pressure

Old Tire		New Tire	
Pressure (psi)	Deflection (in)	Pressure (psi)	Deflection (in)
80	0.296	80	0.280
100	0.232	100	0.238
120	0.206	120	0.225

It can be seen that as the pressure increases in both the old and new tire, the vertical deflection decreases. At a pressure of 80psi, the old tire deflected 0.016in more than the new tire, whereas at pressures of 100psi and 120psi, the new tire deflected more, 0.006in and 0.020in respectively.

Tire Lateral Stiffness

The difference between each before and after 35lb load measurement was averaged for the three runs of each tire. Then the data was averaged for both the old and new tire. Then a graph of lateral deflection versus pressure for the old tire, new tire, and both tires was created using Microsoft Excel (See Figure 3).

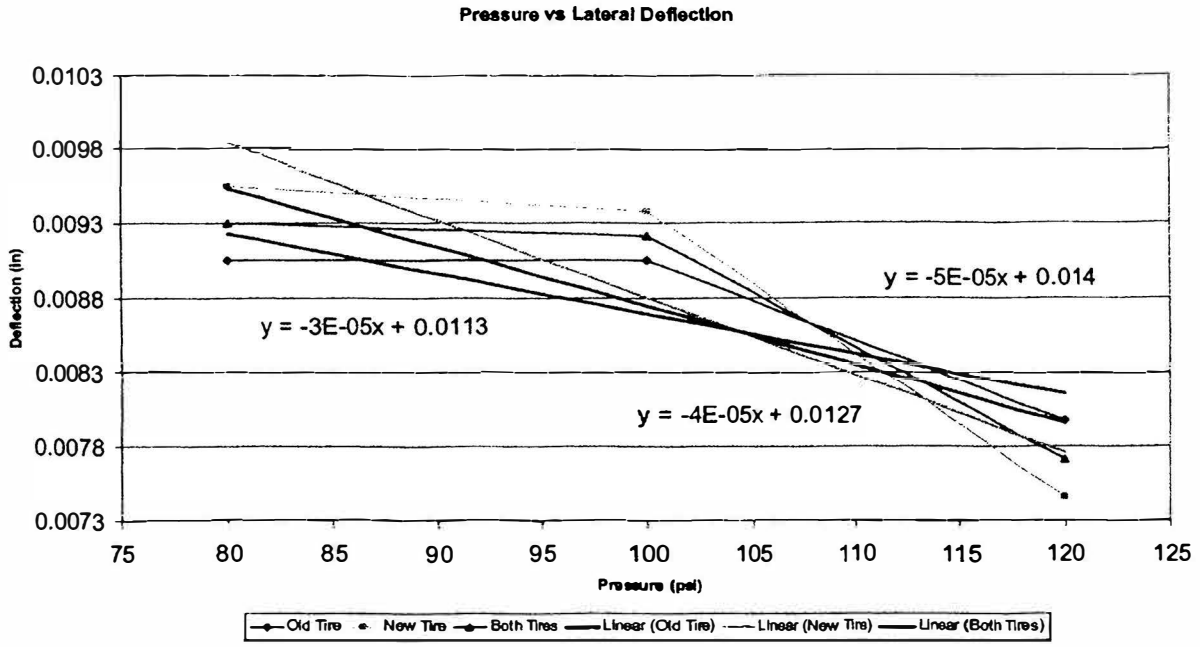

Figure 3: Pressure vs Lateral Deflection

A linear regression equation for the lateral deflection dependent on pressure was then found for data from the old tire, new tire, and both tires. The constants (C_1 and C_2) for the equation of both tires (Equation 1) are given in Table 2.

Table 2: Lateral Deflection Constants

C_1	C_2
-3.958E-05	0.012653

Equation 1: Lateral Deflection Dependent on Pressure

$$D = C_1 \bullet P + C_2,$$

The variables are described as follows: D = lateral deflection equation, P = pressure, and C_1 and C_2 are constants. This equation was used to formulate the lateral stiffness equation, k equation (Equation 2), which was used for the coefficient of rolling resistance analysis.

Equation 2: *k* Equation

$$k = \frac{3\ 5}{D} = \frac{35}{C_1 \bullet P + C_2}$$

The variables are described as follows: k = lateral stiffness equation, 35 = lateral load applied to the tires during the experiment, and D = lateral deflection equation (Equation 1).

Tire Contact Patch

Average elliptical diameters were calculated at each load from the three runs. For each pressure, plots of the contact patch were created, varying with load using Microsoft Excel.

Figure 4 shows the contact patch plot for an old tire at 80psi.

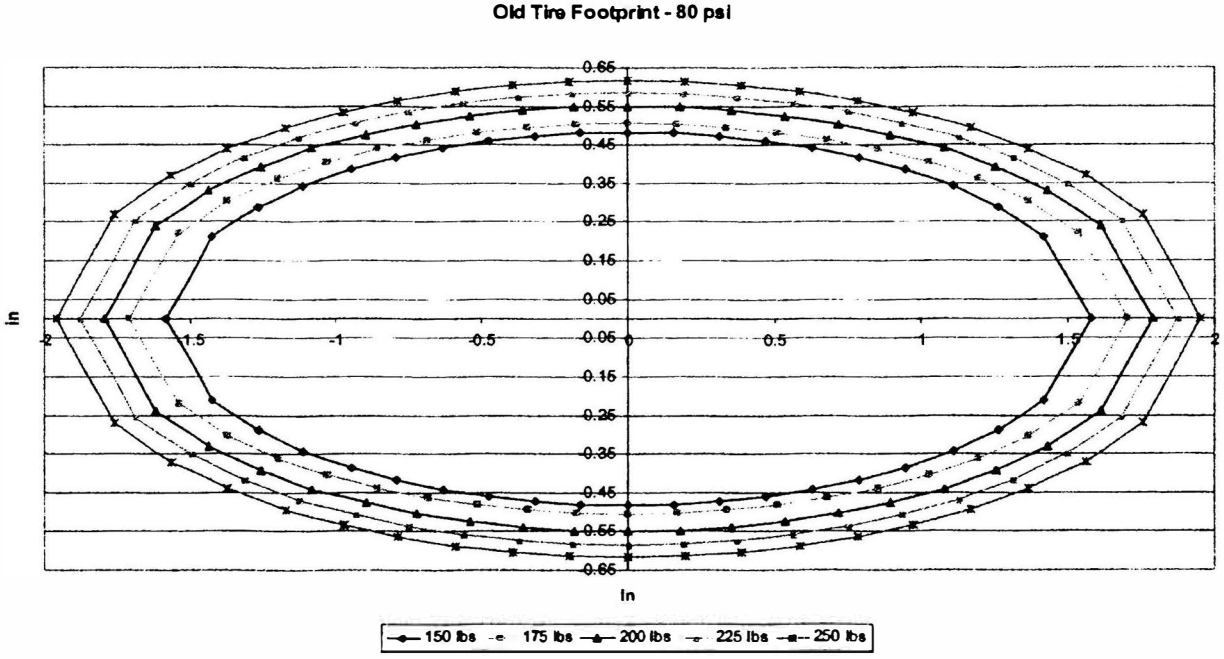

Figure 4: Old Tire Footprint - 80psi

Similar graphs were seen for pressures of 100psi and 120psi as well as for all pressure graphs for the new tire. As the load on the tires increased, the contact patches became larger. Table 3 displays the average a and b values for the contact patch of the old tire varying with pressure and load. The variables a and b are the elliptical diameters; a in the y-direction and b in the x-direction.

Table 3: Old Tire Elliptical Diameters

	Pressure - 80 psi		Pressure - 100 psi		Pressure - 120 psi	
Load	a	b	a	b	a	b
150	0.483	1.578	0.451	1.506	0.444	1.408
175	0.505	1.707	0.477	1.592	0.455	1.511
200	0.550	1.793	0.514	1.678	0.484	1.593
225	0.585	1.870	0.534	1.762	0.512	1.648
250	0.616	1.952	0.570	1.831	0.533	1.729

A table was created listing the average a and b values for the contact patch of the new tire varying with pressure and load (See Table 4).

Table 4: New Tire Elliptical Diameters

	Pressure - 80 psi		Pressure - 100 psi		Pressure - 120 psi	
Load	a	b	a	b	a	b
150	0.484	1.604	0.431	1.526	0.401	1.410
175	0.508	1.700	0.450	1.638	0.442	1.527
200	0.559	1.794	0.503	1.657	0.477	1.578
225	0.598	1.863	0.518	1.745	0.501	1.639
250	0.617	1.975	0.547	1.828	0.515	1.747

For the most part, the old tire elliptical diameters were greater than those of the new tire. A linear regression equation for the length of the contact patch dependent on pressure and vertical load, b equation (Equation 3), was found for both the old and new tire.

Equation 3: b Equation

$$b = C_1 \bullet P + C_2 \bullet W + C_3$$

The variables are described as follows: b = contact patch length, P = pressure, W = load, and C_1, C_2, and C_3 are constants.

Table 5 shows the values for the constants C_1, C_2, and C_3 for both the old and new tires.

Table 5: b Equation Constants

	C_1	C_2	C_3
Old Tire	-0.0051	0.0033	1.5151
New Tire	-0.0052	0.0032	1.5595

This b equation was used for the coefficient of rolling resistance analysis.

Rolling Resistance Coefficient (C_{rr})

For calculations of the rolling resistance coefficient, the flexible tire model (1) was used. The k (Equation 2) and b (Equation 3) equations from the lateral stiffness and contact patch experiments were used. The lateral motion of the tire can be attributed to flexing and/or sliding. There is a critical value δ_C, where the lateral motion of the tire is taken up either by flexing only or flexing and sliding. If the value of $b\sin(\theta) < \delta_C$, then the following equation (Equation 4) for C_{rr}' can be used.

Equation 4: C_{rr} Equation for $b\sin(\theta) < \delta_C$

$$C_{rr}' = \left(1 + \frac{kb\sin(\theta)}{W}\right) C_{rr}$$

The variables are described as follows: C_{rr}' = rolling resistance coefficient, k = lateral stiffness, b = contact patch length, W = load, θ = tire misalignment angle, and C_{rr} is explained by Equation 5.

Equation 5: C_{rr} Equation varied with Pressure

$$C_{rr} = 49.367\left(\frac{P}{100}\right)^{0.3072}\left[19 - \sqrt{19^2 - \frac{2299.7}{19.58 + (5975)(P)}}\right]$$

The variables are described as follows: C_{rr} = rolling resistance coefficient varied with pressure and P = pressure. If the value of $b\sin(\theta) > \delta_C$, then the following equation (Equation 6) for C_{rr}' can be used.

Equation 6: C_{rr} Equation for $b\sin(\theta) > \delta_c$

$$C_{rr}' = C_{rr} + \mu C_{rr} + \left(\frac{b\sin(\theta) - \frac{\mu W}{k}}{b\cos(\theta)} \right)$$

The variables are described as follows: C_{rr}' = rolling resistance coefficient, k = lateral stiffness, b = contact patch length, $\mu = 0.8$ (friction coefficient), W = load, θ = tire misalignment angle, and C_{rr} is explained by Equation 5. Equations 4 through 6 were used to create the following plots: C_{rr} versus theta, C_{rr} versus load, and C_{rr} versus pressure.

C_{rr} versus Theta

Two plots of rolling resistance coefficient (C_{rr}) versus the tire misalignment angle (theta) were created for both the old and new tire. The first plot, Figure 5, is the graph of C_{rr} versus theta for the old tire with pressure set at 100psi and constant load lines.

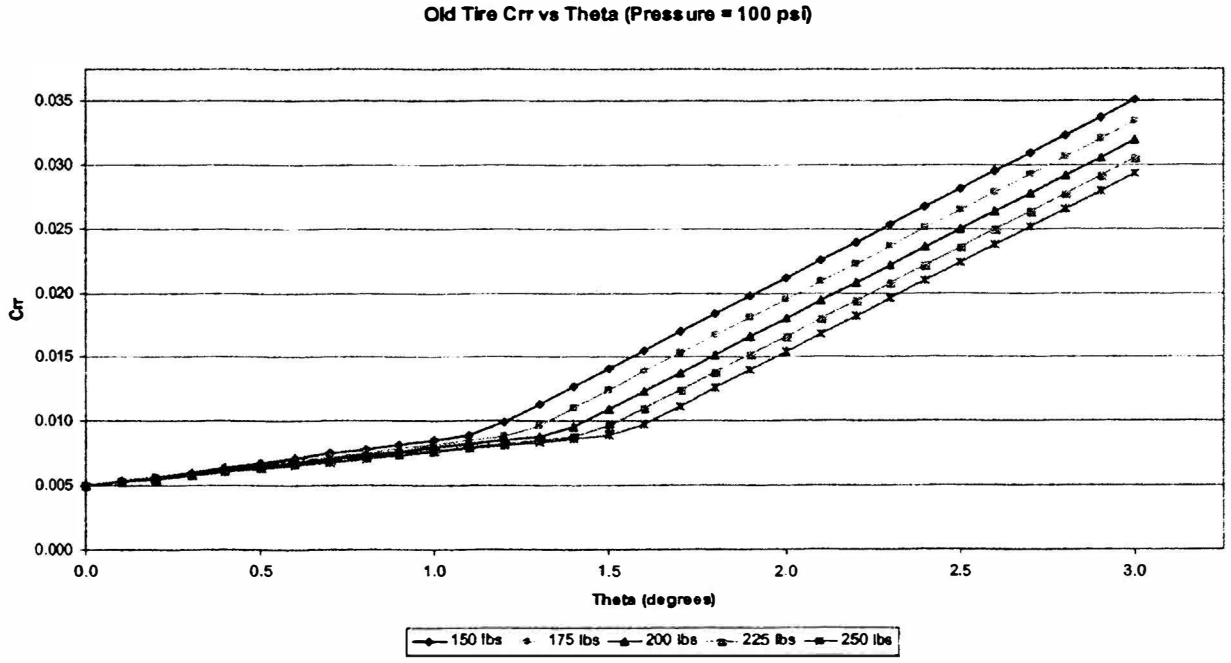

Figure 5: Old Tire C_{rr} vs Theta (Pressure = 100psi)

As can be seen, the C_{rr} increased with increasing values of the misalignment angle, theta. The slopes of these lines decreased with load. With a misalignment angle between 1 and 1.5 degrees, the slopes of C_{rr} versus theta lines increased. Essentially, a tire can have a larger misalignment angle at higher loads. A similar graph was seen for the new tire.

The second plot, Figure 6, is the graph of C_{rr} versus theta for the old tire with load set at 200lbs and constant pressure lines.

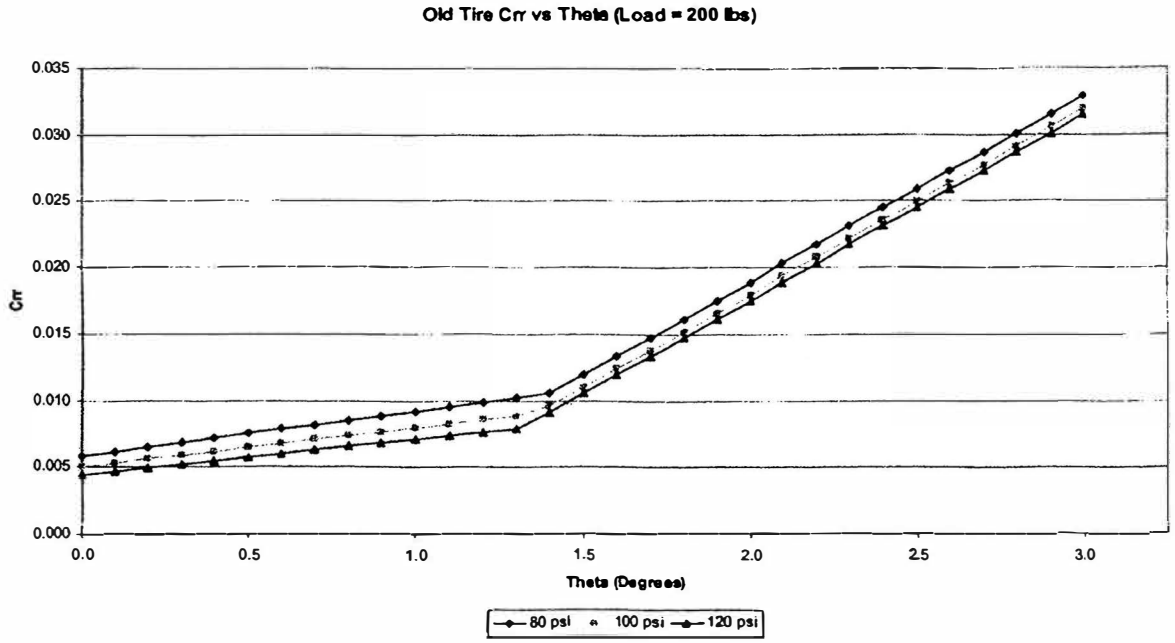

Figure 6: Old Tire C_{rr} vs Theta (Load = 200lbs)

As can be seen, the C_{rr} increased with increasing values of the misalignment angle, theta. The slopes of these lines decreased with pressure. With a misalignment angle between 1.25 and 1.5 degrees, the slopes of C_{rr} versus theta lines increased. Essentially, a tire can have a larger misalignment angle at higher pressures. A similar graph was seen for the new tire.

C_{rr} versus Load

Two plots of rolling resistance coefficient (C_{rr}) versus load were created for both the old and new tire. The first plot, Figure 7, is the graph of C_{rr} versus load for the old tire with a misalignment angle of 1 degree and constant pressure lines.

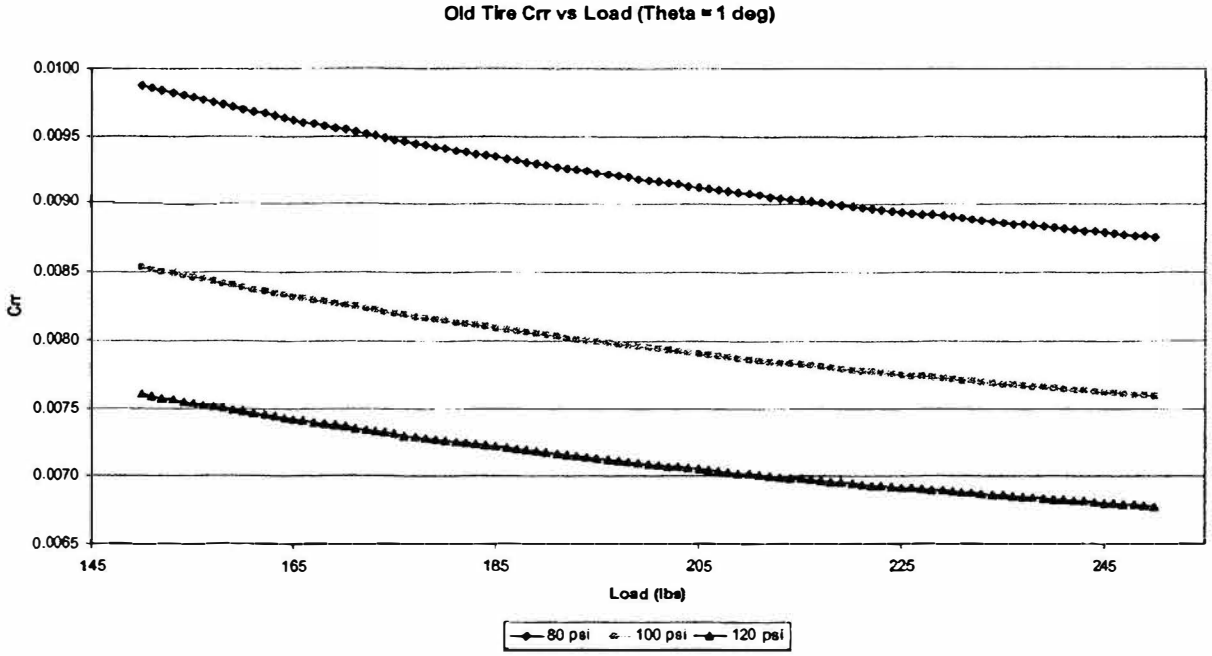

Figure 7: Old Tire C_{rr} vs Load (Theta = 1deg)

As can be seen, the C_{rr} decreased with increasing load and increasing pressure. A similar graph was seen for the new tire. The second plot, Figure 8, is the graph of C_{rr} versus load for the old tire with pressure set at 100psi and constant theta lines.

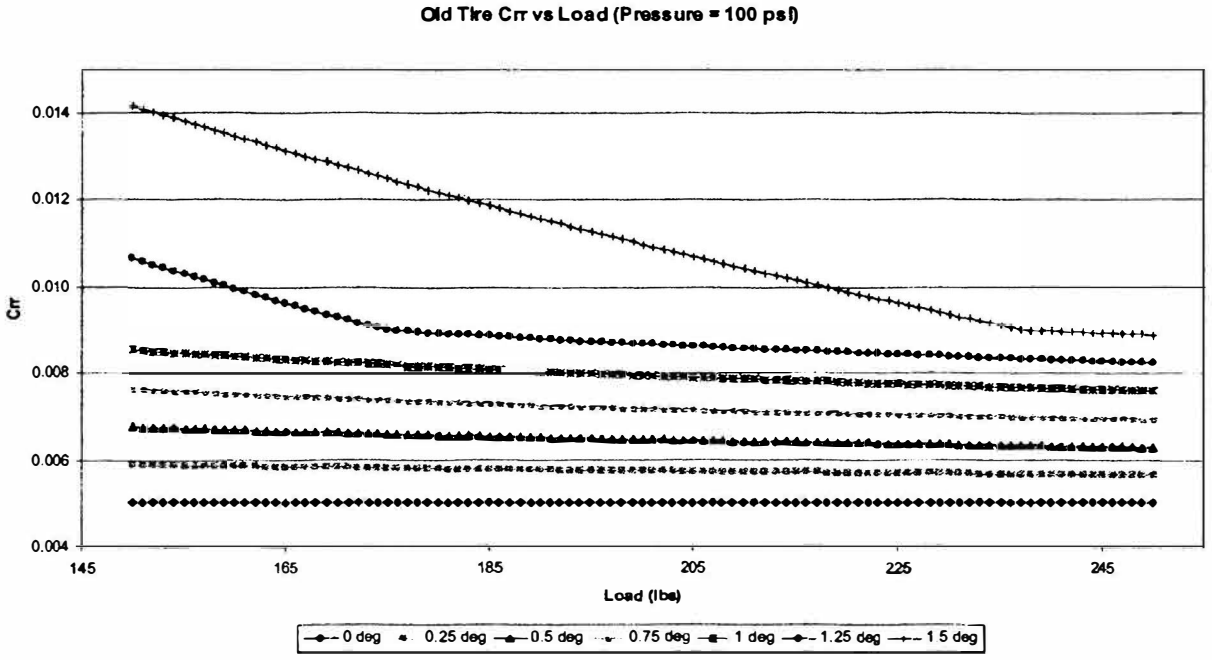

Figure 8: Old Tire C_{rr} vs Load (Pressure = 100psi)

As can be seen, the C_{rr} decreased with increasing load and decreasing values of the misalignment angle. For low values of misalignment angle, 0 to 1 degree, the C_{rr} values are fairly constant. For high values of

misalignment angle, greater than 1 degree, the C_{rr} lines have a very high decreasing slope. A similar graph was seen for the new tire.

C_{rr} versus Pressure

Two plots of rolling resistance coefficient (C_{rr}) versus pressure were created for both the old and new tire. The first plot, Figure 9, is the graph of C_{rr} versus pressure for the old tire with a misalignment angle of 1 degree and constant load lines.

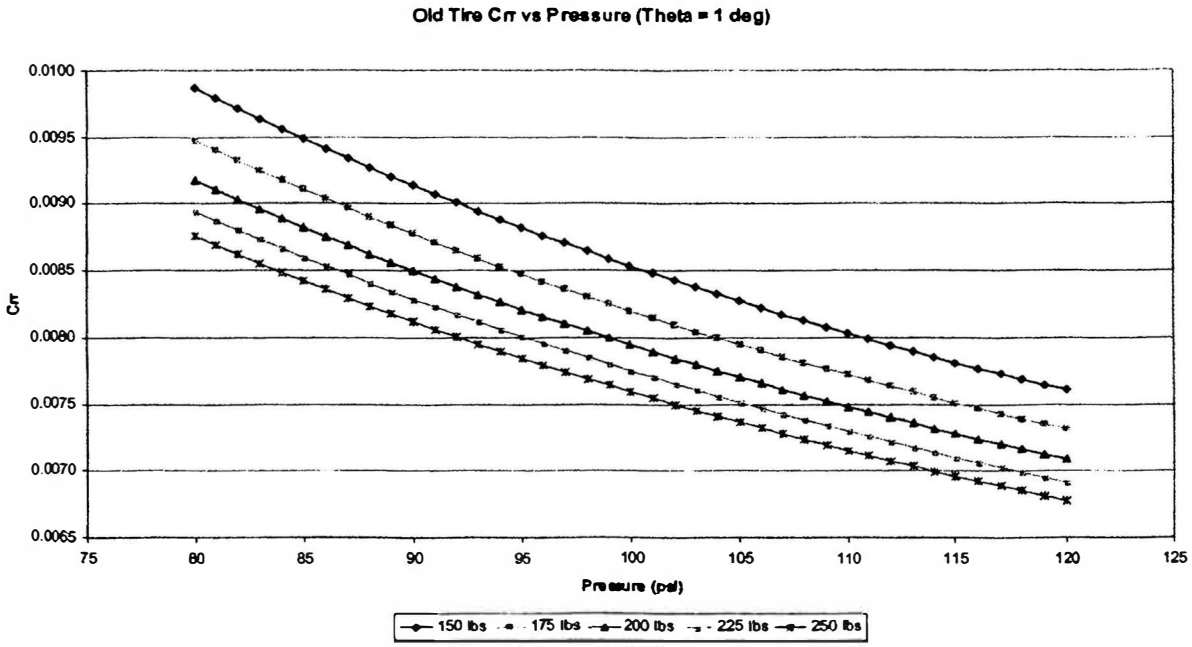

Figure 9: Old Tire C_{rr} vs Pressure (Theta = 1deg)

As can be seen, the C_{rr} decreased with increasing pressure and increasing load. A similar graph was seen for the new tire. The second plot, Figure 10, is the graph of C_{rr} versus pressure for the old tire with load set at 200lbs and constant theta lines.

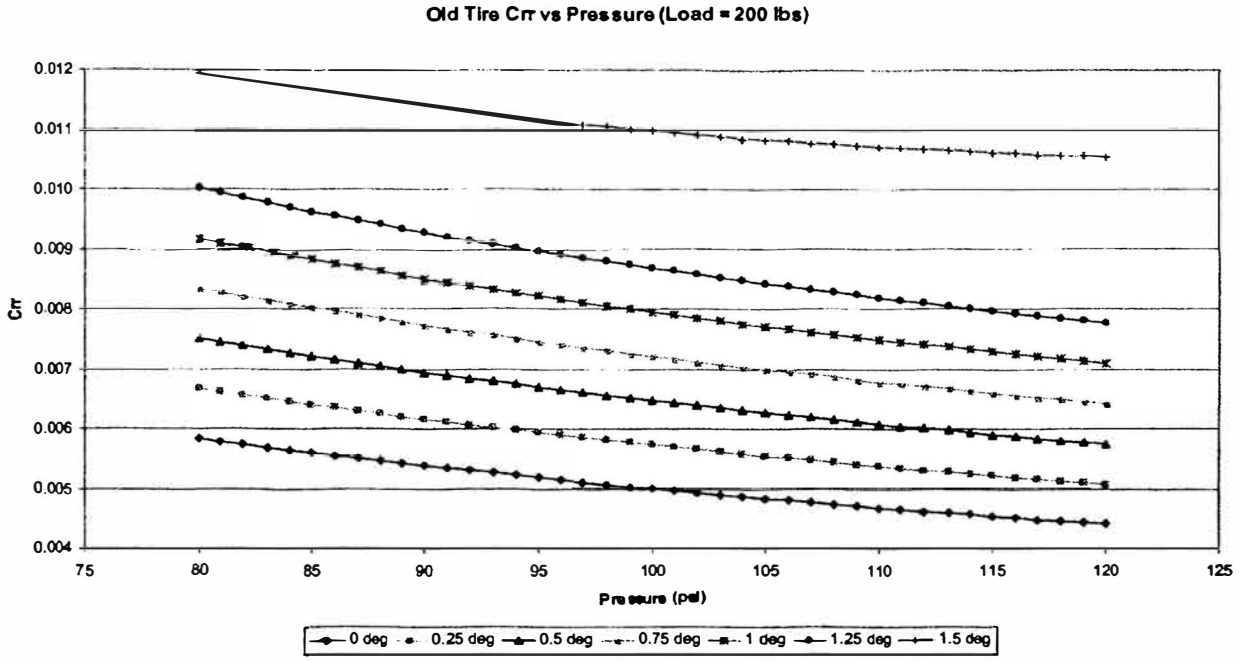

Figure 10: Old Tire C_{rr} vs Pressure (Load = 200lbs)

As can be seen, the C_{rr} decreased with increasing pressure and decreasing values of the misalignment angle. At misalignment angles above 1.25 degrees, there is a high jump in coefficient of rolling resistance. A similar graph was seen for the new tire.

Conclusions

The main goal of this project was to better understand the properties of the Bridgestone Ecopia tires used by the UMR Solar Car Team. Two objectives were realized through this project. The first was to see how the tire deflected vertically with increased load. The second was to be able to better describe the coefficient of rolling resistance of the tires. As expected, with decreasing pressure and increasing load, the vertical deflection of the tire increased. Also, with decreasing pressure and increasing load, the tire contact patch increased in size. The main conclusion that can be reached from the coefficient of rolling resistance results is that the tires should not have a misalignment angle greater than 1 degree to keep the coefficient of rolling resistance down.

Acknowledgements

I am especially grateful to my research advisor, Dr. Doug Carroll, the main faculty advisor for the UMR Solar Car Team. He gave me much needed advice, encouragement, and scientific insights. I would also like to thank Jeff Thomas, the Mechanics of Materials Lab Instructor, for helping me understand the inner workings of the equipment used for the experiments. And finally, I would like to thank the UMR Solar Car Team for allowing me to pursue this project.

References

1. Carroll, Douglas R. The Winning Solar Car: A Design Guide for Solar Race Car Teams. Pennsylvania: SAE International, 2003.